

Synthetic Biology Makes Polymer Materials Count

Hannes M. Beyer, Raphael Engesser, Maximilian Hörner, Julian Koschmieder, Peter Beyer, Jens Timmer, Matias D. Zurbriggen, and Wilfried Weber*

Synthetic biology applies engineering concepts to build cellular systems that perceive and process information. This is achieved by assembling genetic modules according to engineering design principles. Recent advance in the field has contributed optogenetic switches for controlling diverse biological functions in response to light. Here, the concept is introduced to apply synthetic biology switches and design principles for the synthesis of multi-input-processing materials. This is exemplified by the synthesis of a materials system that counts light pulses. Guided by a quantitative mathematical model, functional synthetic biology-derived modules are combined into a polymer framework resulting in a biohybrid materials system that releases distinct output molecules specific to the number of input light pulses detected. Further demonstration of modular extension yields a light pulse-counting materials system to sequentially release different enzymes catalyzing a multistep biochemical reaction. The resulting smart materials systems can provide novel solutions as integrated sensors and actuators with broad perspectives in fundamental and applied research.

Synthetic biology enables the rational design of biological systems by leaning toward well-established design principles of complementary fields such as electrical engineering or control theory.^[1–5] Including quantitative understanding into the design phase of synthetic constructions led to biological systems capable of performing complex computational operations such as oscillation^[6] and synchronized genetic clocks,^[7] or genetic counting of molecular events.^[8] Such systems resulted in applications like the multi-input-based discrimination of cancer and benign cells,^[9] open- and closed-loop-regulated disease control circuits,^[10,11] or

new approaches in fine chemical and drug production.^[12] Along the rapid development of the field increasing demand for biological building blocks with switch-like function arose, acting as trigger-induced actuators within biological circuits. Canonical chemical inducers such as small molecules triggering biological events have paved the development of many proof-of-concept systems yet suffer from inherent drawbacks such as diffusion within the sample volume, lack of reversibility, or toxic side effects. As a consequence of this demand, synthetic biology has merged with optogenetics to engineer novel actuators for controlling biological functions in response to light yielding in unmatched spatial and temporal resolution of control. Having originally emerged from neurosciences to precisely stimulate neurons, this new wave of optogenetics has resulted in light-respon-


sive switches to control cellular events along the whole signal transduction chain, from cell surface receptors to gene expression control (www.optobase.org).^[13,14]

In this work, we devise a design concept of how computational systems inspired by synthetic biology can be transferred from engineered living cells to polymer materials. With this design concept we advance polymer materials from single stimulus responsiveness^[15] to multi-input-processing sensor- and actuator systems. We exemplify this concept by the synthesis of a light-responsive biohybrid materials system that counts the number of input light pulses and releases output molecules specific to the number of light pulses detected. We chose a modular design that discriminates between one and two input light pulses. The material accommodates two main biological subsystems interfacing light pulse perception and counting (**Figure 1**). To sense light, we engineered a variant of the *Arabidopsis* red light photoreceptor phytochrome B (amino acids 1–651, PhyB) covalently conjugated with the linear tetrapyrrole chromophore phycocyanobilin (PCB, **Figure 1a**). PhyB binds a modified phytochrome-interacting factor 6 (amino acids 1–100, designated as PIF) upon illumination with 660 nm or white ambient light (PhyB_{FR}-form). This PhyB_{FR}/PIF interaction reverses under 740 nm light (PhyB_R-form, **Figure 1a**,^[16]). The heterodimerization pair has found broad application in a multitude of cellular synthetic biology applications.^[16–19] To enable the material to count over several light pulses, we needed to implement a subsystem capable of storing information (**Figure 1b**). We utilized a peptide (TEV cleavage site, TCS) that is irreversibly cleaved by the tobacco etch mosaic virus protease (TEV) to capture the memory event. To wire the cleavage

Dr. H. M. Beyer, Dr. M. Hörner, Dr. J. Koschmieder, Prof. P. Beyer, Prof. W. Weber
Faculty of Biology
SGBM – Spemann Graduate School of Biology and Medicine
BIOSS – Centre for Biological Signalling Studies
University of Freiburg
79085 Freiburg, Germany
E-mail: wilfried.weber@biologie.uni-freiburg.de

Dr. R. Engesser, Prof. J. Timmer
Institute of Physics
University of Freiburg
79085 Freiburg, Germany

Prof. M. D. Zurbriggen
Institute of Synthetic Biology and CEPLAS
Heinrich-Heine-Universität Düsseldorf
40225 Düsseldorf, Germany

 The ORCID identification number(s) for the author(s) of this article can be found under <https://doi.org/10.1002/adma.201800472>.

DOI: 10.1002/adma.201800472

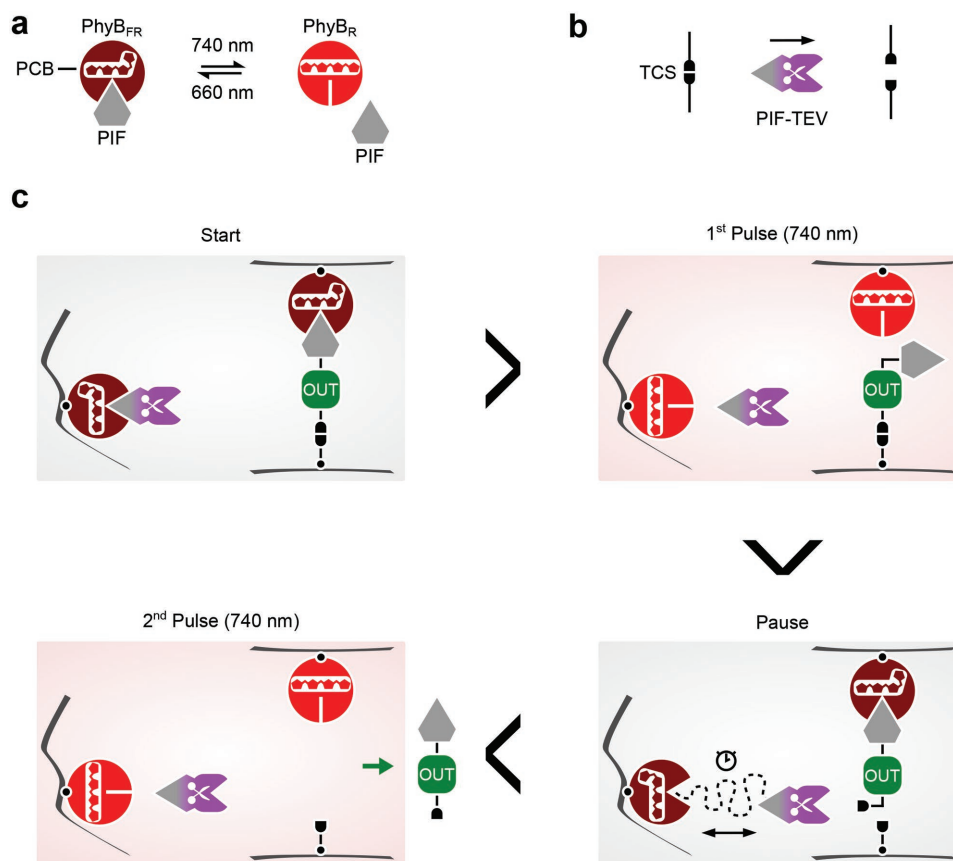


Figure 1. Design of the light pulse-counting materials system. a) The photoreceptor PhyB uses the chromophore PCB to sense red and far-red light. Under 660 nm or white light, PhyB_{FR} binds PIF. This interaction is reversed under 740 nm light when the photoreceptor converts to PhyB_R. b) The TEV protease cleaves a peptide containing the TEV cleavage site (TCS). TEV is fused to PIF via an mCherry linker. c) Molecular composition and mode of function of the light pulse-counting materials system. Start: OUT is bound to a polymer material via PhyB_{FR}/PIF and via TCS. PIF-TEV is polymer-coupled via PhyB_{FR} spatially separated from OUT (Figure S1 for a detailed setup, Supporting Information). 1st Pulse: The first 740 nm light pulse triggers release of PIF-TEV while OUT remains polymer-bound via TCS. Pause: In the pause between the pulses (at 660 nm or white background light) the output rapidly rebinds the polymer via PhyB_{FR}/PIF (due to its TCS-mediated proximity) while the recapture of PIF-TEV to PhyB_{FR} relies on a slower diffusion-based process. During this phase, PIF-TEV cleaves TCS. 2nd Pulse: The second 740 nm light pulse subsequently releases OUT as TCS is already cleaved.

of the TCS peptide to the light input signal, we fused TEV to PIF via the fluorescent protein mCherry for visualization and quantification. We termed this construct PIF-TEV.

Figure 1c depicts the composition and mode of function of the light pulse-counting materials system (Start). First, we coupled an output molecule (OUT) – to be released after the perception of two light pulses – via two parallel bonds to the polymer material. One bond consisted of the TCS peptide, the other of the PhyB_{FR}/PIF interaction. In this configuration, OUT can only be released from the polymer matrix when both bonds open, what requires the sequential or simultaneous activity of PIF-TEV and 740 nm light. Next, we immobilized PIF-TEV to polymer-bound PhyB. To trigger OUT release only after two light pulses were administered, we controlled the presence of PIF-TEV with the first 740 nm light pulse via PhyB_{FR}-dependent immobilization of PIF-TEV to the polymer spatially separated from the OUT-containing subsystem (see Figure S1 for the detailed experimental setup in the Supporting Information).

The counting cycle starts with the assembled materials system under background illumination (white or 660 nm light, Figure 1c, Start). The first 740 nm input light pulse releases

PIF-TEV, while OUT remains polymer-bound via the TCS (Figure 1c, 1st Pulse). In the pause between the first and second light pulse, the PIF anchor of OUT rebinds the polymer. This rebinding is expected to occur rapidly, as PIF remained in close proximity due to the TCS bond. However, rebinding of PIF-TEV relies on a slower diffusion mechanism, leading to TCS cleavage over time (Figure 1c, Pause). The administration of the second light pulse, reversing the PhyB_{FR}/PIF interaction, finally releases OUT from the polymer (Figure 1c, 2nd Pulse).

The building blocks for the light pulse-counting materials system were synthesized in *E. coli*. PhyB (amino acids 1-651) was fused to the biotinylation motif AviTag (PhyB-AviTag,^[20]) for coupling to streptavidin-functionalized polymers. As output (OUT), we chose the enhanced green fluorescent protein (eGFP) and fused its C-terminus to PIF and its N-terminus to the TCS and AviTag to allow divalent binding to PhyB- and streptavidin-functionalized polymers, respectively (AviTag-TCS-eGFP-PIF). See Figure S2a–e (Supporting Information) for production and characterization and Figure S3 (Supporting Information) for stability assessment of the components. Similarly, we produced PIF-TEV and immobilized it to polymer-bound PhyB-AviTag.

To obtain a parameter space in which the light pulse-counting materials system is functional, we first determined the characteristic curves of the individual building blocks and next used a quantitative mathematical model to predict the overall performance.

We used nonlinear ordinary differential equations derived from mass action kinetics and estimated the unknown model parameters by calibrating the model to the following experiments (Figure 2a–d) using a maximum likelihood approach (see the Text in the Supporting Information for the detailed

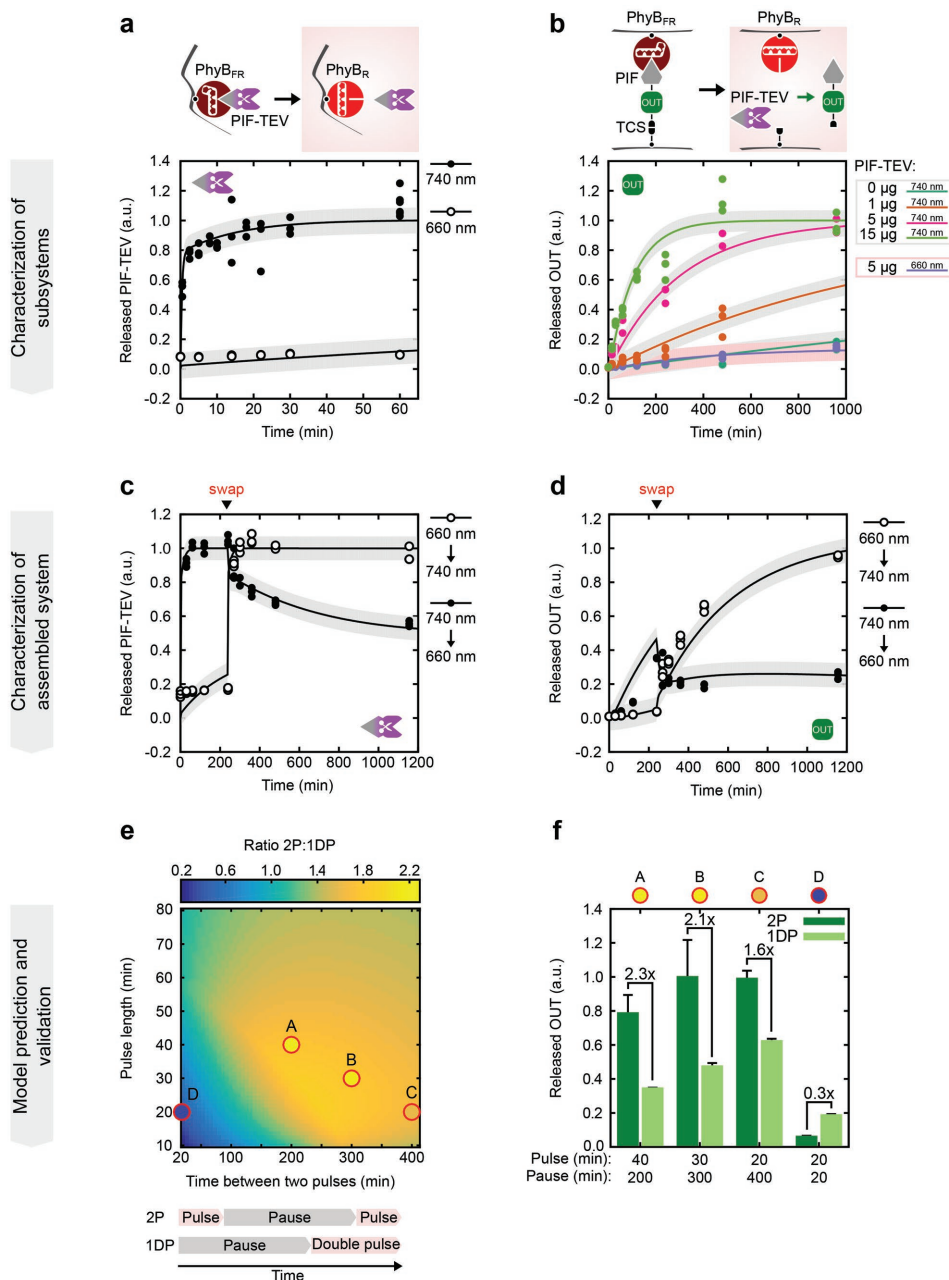


Figure 2. Quantitative characterization of the individual building blocks to calibrate the mathematical model. a) PIF-TEV bound to streptavidin-functionalized agarose via biotinylated PhyB_{FR} was incubated under 660 or 740 nm light and the release of PIF-TEV was monitored. b) PIF-eGFP-TCS bound to streptavidin-functionalized agarose via biotinylated PhyB_{FR} and biotinylated TCS was incubated with indicated amounts of PIF-TEV and the release of OUT (eGFP) was monitored under 660 or 740 nm light. c,d) The complete light pulse-counting polymer material was assembled by combining the modular components from (a) and (b). PIF-TEV c) and OUT d) release and recapture were monitored under 660 or 740 nm light (wavelength swap after 4 h, arrowhead). e) Heat map showing the model-predicted OUT signal ratio of light pulse-counting materials systems that received two pulses of 740 nm light (2P) versus only one pulse of double illumination duration (1DP). Where the basal output signal (without 740 nm pulse) was simulated to be higher than the signal obtained from the 1DP configuration, the basal signal was used for normalization. f) Validation experiments showing the mean values of 2P and 1DP samples at the duty points indicated by the color-coded circles in (e). In (a–d), nonaveraged single point measurement values of at least triplicate experiments are shown. The curves represent the model fits. The shaded error bands correspond to one standard deviation.

description of the mathematical model). First, we measured the characteristic curve for light-dependent PIF-TEV release: 2 nmol PhyB-AviTag coupled to streptavidin-functionalized agarose were loaded with saturating amounts of PIF-TEV under 660 nm illumination for 1 h to allow binding. Subsequently, the release of PIF-TEV in response to illumination with 660 or 740 nm light was monitored for 1 h (Figure 2a). Next, we determined the characteristic curve for TCS cleavage by PIF-TEV and recorded the release of the output molecule eGFP: AviTag-TCS-eGFP-PIF (67 pmol) was mixed with PhyB-AviTag (2 nmol) under 660 nm illumination and subsequently coupled to streptavidin-functionalized agarose. After washing, the release kinetics of eGFP as a function of added PIF-TEV (to simulate the release of PIF-TEV by the first 740 nm light pulse) were determined under 740 and 660 nm illumination for 16 h (Figure 2b). These results show that OUT release indeed requires the activity of both PIF-TEV and 740 nm light, as OUT remained bound to the material under 660 nm light albeit in presence of PIF-TEV (red-shaded line). Finally, we assembled the complete materials system (as depicted in Figure 1c, Start) and measured the release kinetics of PIF-TEV and eGFP under alternating 660 and 740 nm light illumination (Figure 2c,d).

We identified the operating range of the light-pulse counting materials system by simulation studies as a function of light pulse length and the duration of the pause. As the criterion for counting capability, we selected the ratio of the output signal after two 740 nm light pulses (2P) versus the signal obtained after only one light pulse of double duration (1DP). A ratio >1 indicated differentiation between one and two light pulses rather than simple integration of the total input signal. The mathematical model predicted the operating space in which the system displayed counting functionality (Figure 2e). These predictions were experimentally validated (Figure 2f; circles in Figure 2e). Validation profile likelihood analysis (See the Text in the Supporting Information,^[21]) for each experimental point confirmed the predicted ratios within the 95% confidence interval (Figure S7b,c, Supporting Information).

Based on this functional validation, we next applied the mathematical model to identify an illumination regime that maximizes the absolute release of OUT after the second light pulse where all light pulses are of identical duration. We simulated the difference of OUT release after the second and the first light pulse over variable pulse and pause lengths (Figure 3a,b). The simulations revealed that extending both time intervals would contribute to an increased output release. We chose a duty point of 60 min pulse and 300 min pause length where we expected OUT release close to saturation (Figure 3b, red point). Subjecting the light pulse-counting materials system with the illumination regime as determined from the simulations, revealed high release of OUT only after the administration of two light pulses (Figure 3a,c). These results indicate that the materials system is capable of releasing an embedded cargo molecule specifically after it has counted two light pulses.

The modular nature of the materials system suggests for a multitude of possible extension, e.g., connection of modules in series, or shunt circuits. Hence, we decided to extend the materials system with an additional module responding in parallel to the release of PIF-TEV upon stimulation of a single light pulse. The here-released molecule would initiate a serial chemical

reaction to be completed by a second molecule released with the second light pulse (Figure 3d–g). We chose to demonstrate this sequential release using two biocatalysts as cargoes to perform the following two-step enzymatic reaction (Figure 3d,e): from 15-*cis*-phytoene to the intermediate product all-*trans*-lycopene (catalyzed by the phytoene desaturase CrtI,^[22]) and subsequently to the final product, the pro-vitamin A, all-*trans*- β -carotene (catalyzed by the lycopene cyclase CrtY,^[23] Figure S4, Supporting Information). In order to release CrtI in response to the first 740 nm light pulse, we extended the materials system by a module comprising a CrtI-PIF fusion protein bound to PhyB_{FR}-coupled agarose (Figure 3d). CrtY was inserted between the TCS and eGFP in the above-described output construct, to be released after the second light pulse (Figure 3d; and Figure S4a, Supporting Information). Both modified enzymes were produced in *E. coli* (see Figure S4b–e for production and characterization, Supporting Information) and subsequently incorporated into the materials system.

To run the two-step reaction, we introduced both enzymes into the light pulse counting materials system (24 nmol PIF-CrtI; 134 nmol CrtY-eGFP-containing output) and started the reaction by applying the first light pulse to release PIF-TEV and PIF-CrtI. PIF-TEV triggered the cleavage of TCS during the pause. Simultaneously, PIF-CrtI initiated the conversion of 15-*cis*-phytoene to all-*trans*-lycopene. The second light pulse, applied after the pause, released CrtY-eGFP to catalyze the reaction of all-*trans*-lycopene into all-*trans*- β -carotene. We analyzed the output release by quantifying the amount of the reaction products (Figure 3f,g), revealing high synthesis of the intermediate product lycopene after the first light pulse and high synthesis of the final product β -carotene after the second pulse. This suggests that the light pulse-counting polymer material is suitable for the sequential release of two different output molecules, specific to the number of input pulses.

In this study, we demonstrate how multi-input-sensing and information-processing materials systems can be synthesized using design concepts and building blocks derived from synthetic biology. The biological origin of the used building blocks implicates inherent functionality under physiological conditions. For example, the binding specificity between PhyB and PIF has evolutionary been optimized to be robust against high concentrations of diverse small and macromolecular compounds present in a physiological background. Similarly, the sensitivity of biomolecular sensors such as the photoreceptor PhyB has evolutionary been shaped to respond to physiologically compatible stimulus concentrations, or light conditions.^[18] These features make biomolecular sensors highly attractive for the synthesis of stimulus-responsive biohybrid materials systems with application in biological environments such as cell and tissue culture, or in vivo. Biomaterials systems, which are able to discriminate between the numbers of light pulses, provide diverse novel opportunities for practical application. For example, the ability to sequentially release different (biomolecular) cargoes by the simple application of a light pulse suits the design of portable analytical devices requiring the sequential addition of reagents and thus overcomes the need for reagent pumps (e.g., ELISA-like formats). Further, polymer materials that sequentially release biomolecules in response to biocompatible stimuli might foster advances as synthetic

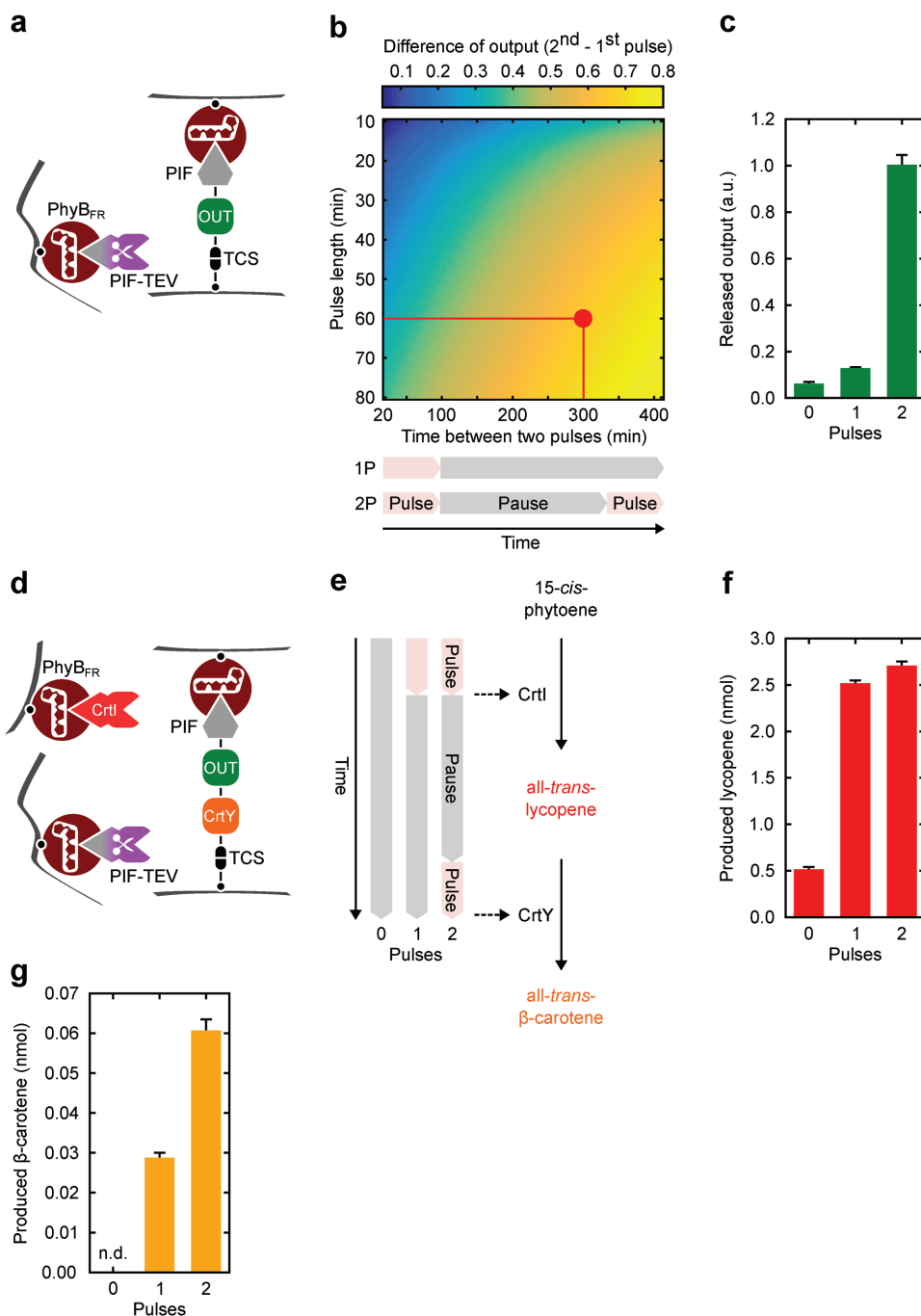


Figure 3. Modular extension of the light pulse-counting materials system. a) Design of the basic light pulse-counting materials system. b) Model-based identification of the duty point for maximizing the absolute release of OUT. The difference of OUT release after the second light pulse and the first pulse was simulated as a function of the pulse- and pause-duration. The duty point chosen is shown in red. c) OUT release of the basic light pulse-counting materials system shown in (a) at the duty point shown in (b). d) Modular extension of the light pulse-counting materials system to control sequential release of biocatalysts. e) Two-step biosynthesis. All-*trans*- β -carotene is synthesized from 15-*cis*-phytoene by the light pulse-controlled sequential release of phytoene-desaturase CrtI (first pulse) and lycopene-cyclase CrY (second pulse). f,g) The light pulse-counting polymer material was extended with PIF-CrtI bound to PhyB-functionalized agarose and CrY fused to the eGFP OUT module as shown in (d). The reaction was started with one 740 nm light pulse (60 min), followed by a pause of 300 min prior to the second light pulse (60 min). After each light pulse, the released enzymes were used to catalyze the respective reaction step and lycopene f) and β -carotene g) were quantified.

extracellular matrix. In such settings, light pulses could be applied for the sequential release of cytokines or growth factors to trigger multistep cell fate decisions frequently desired in

stem cell lineage control.^[24] Similarly, counting materials could open new avenues in drug delivery for administering multiple drug doses on command, a limitation of current single-release

stimulus-responsive drug depots.^[25] One may also combine optically responsive depots with recently described devices for the remote control of implanted red light-responsive optogenetic switches.^[26]

About 15 years ago, pioneering work at the interface of biological and engineering disciplines shaped the foundations of synthetic biology.^[27,28] The modular, model-guided assembly of biological building blocks to networks with computational capacity has yielded in a vast array of applications addressing bottlenecks in the biomedical, energy, environmental, and chemical sectors.^[29] Given this array of networks and applications with the opportunity to transfer tools and design concepts from synthetic biology to materials sciences, now provides novel perspectives for the synthesis and application of information-sensing and -processing materials systems.

Experimental Section

Protein Design, Production, Purification, and Analytics: A detailed cloning strategy for the expression constructs as well as methods for producing, purifying, and quantifying the biomolecules is described in the Supporting Information.

Material Synthesis and Characterization: The PhyB/PIF-TEV subsystem was synthesized by coupling PhyB to cross-linked agarose. To this aim, cross-linked agarose (10 μ L) covalently functionalized with streptavidin (Novagen, size: 40–165 μ m, 240 nmol free biotin-binding capacity per mL, as determined using a Biotin Quantitation Kit, Pierce) were incubated with 2 nmol biotinylated PhyB in a total volume of 10 mL assembly buffer (100 \times 10⁻³ M Tris/HCl, 150 \times 10⁻³ M NaCl, 1% BSA, 1 \times 10⁻³ M 2-mercaptoethanol (2-ME), pH 8.0). The reaction was rotated at 4 °C for 45 min and washed subsequently with assembly buffer for 10 min. An at least threefold molar excess of PIF-TEV was added and the material was incubated at 660 nm light for 1 h at room temperature (RT) while shaking. The material was subsequently washed 3 \times 30 min with assembly buffer at 660 nm light while shaking.

The eGFP output containing subsystem was synthesized by mixing biotinylated PhyB and biotinylated cargo in a molar ratio of 30:1 in assembly buffer to avoid excess of cargo protein. The protein mixture was illuminated with 660 nm light for 1 h at RT, shaking. Subsequently, streptavidin-functionalized agarose (10 μ L, see above) was added per 2 nmol of biotinylated PhyB and the sample was incubated for 45 min at RT with 660 nm light illumination while shaking. Three steps of washing were performed (660 – 740 – 660 nm light) for 45 min each at RT, while shaking to remove unbound protein.

CrtI/CrtY-loaded materials were synthesized with a modified assembly buffer (50 \times 10⁻³ M Na₂HPO₄, 150 \times 10⁻³ M NaCl, 5 \times 10⁻³ M MgCl₂, 1% BSA, 1 \times 10⁻³ M 2-ME, pH 8.0) where BSA, or BSA and 2-ME were omitted in the last washing step for CrtY and CrtI-loaded materials, respectively.

For synthesizing the complete light pulse-counting polymer material, the above-described subsystem materials were combined in one system separated by a permeable polymer membrane (Merck Millipore, MultiScreen-MESH Filter Plate, 20 μ m) in order to achieve a diffusion-based PIF-TEV cleavage mechanism. Both materials building blocks were used in equimolar ratios referring to the amount of PhyB-AviTag (typically corresponding to 2.4 nmol biotin-binding capacity of the agarose-streptavidin material). For the CrtY-based material, the amount of the OUT-containing material was doubled. Additionally, agarose-coupled PhyB-AviTag (1 nmol) was added. The total volume in each well was adjusted (500 μ L) with the respective assembly buffer and samples were illuminated with 660 nm and/or 740 nm light as indicated.

Tailor-made light boxes housing LEDs (Roithner, cat. No. LED660N-03, LED740_01AU) were used for illumination. Samples were illuminated with 660 or 740 nm light with an intensity of 100 or

110 μ mol quanta s⁻¹ m⁻², respectively. Light intensities were calibrated using an AvaSpec-ULS2048 Fiber Optic Spectrometer (Avantes).

Supporting Information

Supporting Information is available from the Wiley Online Library or from the author.

Acknowledgements

The authors thank J. Schmidt, D. Schächtele, and J. Meßner (University of Freiburg) for constructing the illumination devices; L. O. Essen (University of Marburg) for plasmids p171 and p83 and C. Voigt (MIT) for plasmid pAL149. They also thank S. Samodelov for critically reading the manuscript. This work was supported by the European Research Council [FP7/2007-2013]/ERC [259043]-CompBioMat and the excellence initiative of the German Federal and State Governments [EXC-294-BIOSS, GSC-4-SGBM].

Conflict of Interest

The authors declare no conflict of interest.

Keywords

biomaterials, materials systems, optogenetics, synthetic biology

Received: January 22, 2018

Revised: February 25, 2018

Published online:

- [1] R. Daniel, J. R. Rubens, R. Sarpeshkar, T. K. Lu, *Nature* **2013**, *497*, 619.
- [2] S. Ausländer, D. Ausländer, M. Müller, M. Wieland, M. Fussenegger, *Nature* **2012**, *487*, 123.
- [3] T. S. Moon, C. Lou, A. Tamsir, B. C. Stanton, C. A. Voigt, *Nature* **2012**, *491*, 249.
- [4] A. L. Slusarczyk, A. Lin, R. Weiss, *Nat. Rev. Genet.* **2012**, *13*, 406.
- [5] A. A. K. Nielsen, B. S. Der, J. Shin, P. Vaidyanathan, V. Paralanov, E. A. Strychalski, D. Ross, D. Densmore, C. A. Voigt, *Science* **2016**, *352*, aac7341.
- [6] Y. Chen, J. K. Kim, A. J. Hirning, K. Josić, M. R. Bennett, *Science* **2015**, *349*, 986.
- [7] T. Danino, O. Mondragón-Palomino, L. Tsimring, J. Hasty, *Nature* **2010**, *463*, 326.
- [8] A. E. Friedland, T. K. Lu, X. Wang, D. Shi, G. Church, J. J. Collins, *Science* **2009**, *324*, 1199.
- [9] Z. Xie, L. Wroblewska, L. Prochazka, R. Weiss, Y. Benenson, *Science* **2011**, *333*, 1307.
- [10] H. Ye, M. Daoud-El Baba, R.-W. Peng, M. Fussenegger, *Science* **2011**, *332*, 1565.
- [11] M. Xie, H. Ye, H. Wang, G. Charpin-El Hamri, C. Lormeau, P. Saxena, J. Stelling, M. Fussenegger, *Science* **2016**, *354*, 1296.
- [12] S. Galanie, K. Thodey, I. J. Trenchard, M. Filsinger Interrante, C. D. Smolke, *Science* **2015**, *349*, 1095.
- [13] K. Kolar, W. Weber, *Curr. Opin. Biotechnol.* **2017**, *47*, 112.
- [14] N. A. Repina, A. Rosenbloom, A. Mukherjee, D. V. Schaffer, R. S. Kane, *Annu. Rev. Chem. Biomol. Eng.* **2017**, *8*, 13.

- [15] M. A. C. Stuart, W. T. S. Huck, J. Genzer, M. Müller, C. Ober, M. Stamm, G. B. Sukhorukov, I. Szleifer, V. V. Tsukruk, M. Urban, F. Winnik, S. Zauscher, I. Luzinov, S. Minko, *Nat. Mater.* **2010**, *9*, 101.
- [16] A. Levskaya, O. D. Weiner, W. A. Lim, C. A. Voigt, *Nature* **2009**, *461*, 997.
- [17] J. E. Toettcher, O. D. Weiner, W. A. Lim, *Cell* **2013**, *155*, 1422.
- [18] K. Müller, R. Engesser, S. Metzger, S. Schulz, M. M. Kämpf, M. Busacker, T. Steinberg, P. Tomakidi, M. Ehrbar, F. Nagy, J. Timmer, M. D. Zubriggen, W. Weber, *Nucleic Acids Res.* **2013**, *41*, e77.
- [19] H. M. Beyer, S. Juillot, K. Herbst, S. L. Samodelov, K. Müller, W. W. Schamel, W. Römer, E. Schäfer, F. Nagy, U. Strähle, W. Weber, M. D. Zurbriggen, *ACS Synth. Biol.* **2015**, *4*, 951.
- [20] S. S. Ashraf, R. E. Benson, E. S. Payne, C. M. Halbleib, H. Grøn, *Protein Expression Purif.* **2004**, *33*, 238.
- [21] C. Kreutz, A. Raue, J. Timmer, *BMC Syst. Biol.* **2012**, *6*, 120.
- [22] P. Schaub, Q. Yu, S. Gemmecker, P. Poussin-Courmontagne, J. Mailliot, A. G. McEwen, S. Ghisla, S. Al-Babili, J. Cavarelli, P. Beyer, *PLoS One* **2012**, *7*, e39550.
- [23] Q. Yu, P. Schaub, S. Ghisla, S. Al-Babili, A. Krieger-Liszkay, P. Beyer, *J. Biol. Chem.* **2010**, *285*, 12109.
- [24] P. Saxena, B. C. Heng, P. Bai, M. Folcher, H. Zulewski, M. Fussenegger, *Nat. Commun.* **2016**, *7*, 11247.
- [25] R. J. Gübeli, D. Hövermann, H. Seitz, B. Rebmann, R. G. Schoenmakers, M. Ehrbar, G. Charpin-El Hamri, M. Daoud-El Baba, M. Werner, M. Müller, W. Weber, *Adv. Funct. Mater.* **2013**, *23*, 5337.
- [26] J. Shao, S. Xue, G. Yu, Y. Yu, X. Yang, Y. Bai, S. Zhu, L. Yang, J. Yin, Y. Wang, S. Liao, S. Guo, M. Xie, M. Fussenegger, H. Ye, *Sci. Transl. Med.* **2017**, *9*, eaal2298.
- [27] T. S. Gardner, C. R. Cantor, J. J. Collins, *Nature* **2000**, *403*, 339.
- [28] M. B. Elowitz, S. Leibler, *Nature* **2000**, *403*, 335.
- [29] T. Kitada, B. DiAndreth, B. Teague, R. Weiss, *Science* **2018**, *359*, eaad1067.